Stem Cell Reports, Volume *8*

Supplemental Information

MAD2L2 Promotes Open Chromatin in Embryonic Stem Cells and Derepresses the *Dppa3* Locus

Ali Rahjouei, Mehdi Pirouz, Michela Di Virgilio, Dirk Kamin, and Michael Kessel

SUPPLEMENTAL INFORMATION

Supplemental Experimental Procedures

Cell culture.
Mad2l2-deficient ESCs carrying an Oct4-GFP ESCs have an insertion of the GFP open reading frame behind the Oct4 enhancers CR I, II and IV, while CR II is deleted (Boiani et al., 2004). GFP expression demarcates the early embryonic epiblast, PGCs, and ESCs, but not the late epiblast. In order to visualize Dppa3 expression we employed BVSC ESCs were generated and provided by M. Saitou (Kyoto University, Japan). ESCs were transfected with Lipofectamine 2000 as recommended, and 8 h after transfection cells were harvested (three independent biological replicates). MEFs were generated and grown as described (Pirouz et al., 2013). DNA damage was induced wit 50 nM mitomycin for 20 min. Histone acetylation was inhibited with Trichostatin A (SIGMA; 250 nM) or SAHA (SIGMA; 10 μm) for eight hours in LIF/2i medium (three independent biological replicates).

Flow cytometry.
Trypsinized cells were labelled with antibodies, washed, and then fixed in methanol (-20 °C). After washing they were resuspended in blocking solution (1% bovine serum albumin, 1% Tween, 22.52 mg/ml glycine in phosphate buffered saline (PBS). Antibodies were applied overnight at 4 °C. Slides were washed three times for 10 minutes with PBS. Secondary antibody was applied and incubated for 60 minutes at room temperature. Slides were washed three times for 10 minutes with PBS.

Cell fractionation.
10^8 cells were pelleted, washed and resuspended in 2 ml of ice-cold NP-40 lysis buffer. Nuclei were pelleted at 120 x g at 4 °C for 10 min, and the supernatant cytoplasmic fraction was saved. Pellet was resuspended in 1 ml low salt buffer + 1% Triton X-100 and incubated on ice for 10 min. Chromatin fraction was pelleted at 120 x *g* at 4 °C for 10 min, and the supernatant nucloplasmic fraction was saved. Chromatin fraction was solved in 125 μl of 0.2 N HCl and neutralized with same volume of Tris-HCl pH8.

Cryosectioning. PGCLC aggregates were harvested, washed, and fixed in 4% formaldehyde (pH 7.4) for 2 hours. Cells were dehydrated by transfer to 10%, 20% and 30% sucrose solutions. Finally, the aggregates were transferred into tissue-tek solution, and frozen on dry ice. Cryo-microtome sections were stored at -80 °C.

RT-PCR. RNA and cDNA were prepared by standard procedures, and amplifications were executed with a Biosystems 7300 Sequence Detection system. All experiments were repeated for at least three times independently, with two technical replicates each. Primers were designed by the primer-blast tools from NCBI. Expression levels were calculated based on Ct values after normalization for GAPDH.

Immunocytochemistry. Cells were cultured on chamber slides (Nuc Lab-Tek), washed with PBS, and rinsed with NP-40/0.2% PBS for 10 min for permeabilization. Washing steps were repeated by PBT. Cells were covered with blocking solution for 60 minutes (1% BSA, 22.52 mg/ml glycine in PBT). The first antibody was applied overnight at 4 °C, and after washing the secondary antibody was applied for 60 minutes. Slides were washed, and mounted in Mounting Medium with DAPI (Vector Laboratories). Samples were documented by confocal (Leica SP3) or Stimulated Emission Depletion (STED) microscopy. ImageJ software (https://imagej.nih.gov/ij/) was used for all image processing and quantifications.

The following primary antibodies were used at dilutions of 1:100 or 1:200: Anti-DPPA3 (Santa Cruz, sc-19878), Anti-H3K9me2 (Abcam, ab6002), Anti-H3K27me3 (Abcam, ab8580), Anti-RNF168 (Santa Cruz, sc-101125), Anti-53BP1 (Santa Cruz, sc-22760), MAD2l2 (Abcam, ab180579). Secondary antibodies were Alexa Fluor 488 (Thermo Fisher, Z25002, Z25302), Alexa Fluor 594 (Thermo Fisher, Z25007, Z25007), Alexa Fluor 647 (Thermo Fisher, Z25308), STAR 635 and STAR 580 (Abberior, Goettingen, 2-0032-051-9).

STED microscopy. The procedure was modified from (Revelo et al., 2014). Immunostained cells were transferred to unpolymerized resin *(p*-toluenesulfonic acid monohydrate/2,4,6-Tris[bis(methoxymethyl)amino]-1,3,5-triazine) in a BEEM capsule. Samples were kept overnight at room temperature to allow penetration of melamine, and were then warmed to 40°C for 24 h. The BEEM capsule was filled to the top with Epon resin (EpoFix kit; Struers), and heated to 60°C for 48 h. Ultrathin sections of 30 or 80 nm were prepared with an ultramicrotome (EM UC6; Leica) and documented by high resolution STED microscopy (TCS SP5; Leica).

ChIP-seq and MeDIP-seq. DNA libraries were produced with the QuantiFluor dsDNA System (Promega), and the size range was determined with the Bioanalyzer 2100 (Agilent). Libraries were amplified and sequenced at 100 bp resolution with an
Illumina HiSeq2000 sequencer. The Illumina software BaseCaller was used for the conversion of sequence images to Fastq files, which were analyzed for quality with the fastx_toolkit. Alignment was performed with bowtie 2 software for Illumina based on the mm10 reference genome. Duplications were removed with RmDup (version 2.0.0). The reference genome was annotated by merging with a Gff3 file. Merged files in combination with the INPUT file were used for peak calling by MACS (version 2.2.2). Methylated areas were recognized by the MEDIPS package of the R software (version 3.2.2) (Weber et al., 2005). Data were visualized by Integrative Genomics Viewer (version 2.3).

RNAseq. Previously reported fastq files (Pirouz et al., 2015) were re-evaluated by alignment with BWA for Illumina, based on mm10 instead of mm9. BAM files were prepared with a procedure similar to ChIP-seq data. Significant changes of gene expression were determined by the two independent methods Cuffdiff and deseq2. Data were visualized by the Visualization-Bioconductor package of the R software.

Supplemental References

Boiani, M., Kehler, J., and Scholer, H.R. (2004). Activity of the germline-specific Oct4-GFP transgene in normal and clone mouse embryos. Methods Mol Biol *254*, 1-34.

Hayashi, K., Ohta, H., Kurimoto, K., Aramaki, S., and Saitou, M. (2011). Reconstitution of the mouse germ cell specification pathway in culture by pluripotent stem cells. Cell *146*, 519-532.

Pirouz, M., Pilarski, S., and Kessel, M. (2013). A critical function of Mad2l2 in primordial germ cell development of mice. PLoS Genet *9*, e1003712.

Pirouz, M., Rahjouei, A., Shamsi, F., Eckermann, K.N., Salinas-Riester, G., Pommerenke, C., and Kessel, M. (2015). Destabilization of pluripotency in the absence of Mad2l2. Cell Cycle *14*, 1596-1610.

Revelo, N.H., Kamin, D., Truckenbrodt, S., Wong, A.B., Reuter-Jessen, K., Reisinger, E., Moser, T., and Rizzoli, S.O. (2014). A new probe for super-resolution imaging of membranes elucidates trafficking pathways. J Cell Biol *205*, 591-606.

Weber, M., Davies, J.J., Wittig, D., Oakeley, E.J., Haase, M., Lam, W.L., and Schubeler, D. (2005). Chromosome-wide and promoter-specific analyses identify sites of differential DNA methylation in normal and transformed human cells. Nat Genet *37*, 853-862.

Supplemental Figures

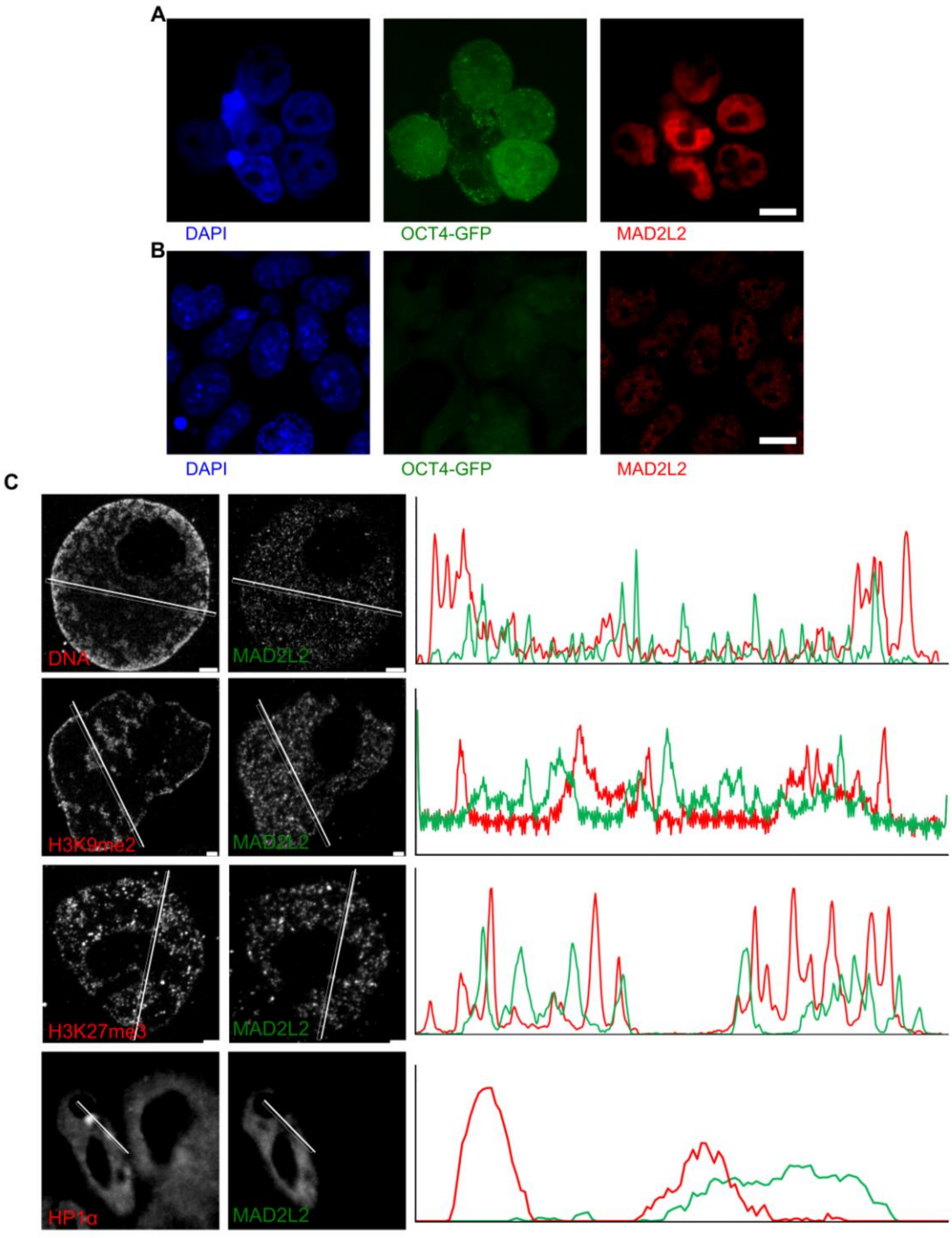

Figure S1 (Related to Figure 1). Downregulation of MAD2L2 Accompanies The Transition from Naive to Primed Pluripotency

(A) High levels of MAD2L2 protein in naive ESCs grown in LIF/2i medium, note heterogeneity of MAD2L2, but not Oct4-GFP expression.

(B) Absence of MAD2L2 protein from EpiLCs, which were generated from ESCs by growth in medium containing activin, bFGF and serum replacement for 6 days. Magnification bars (A,B) = 10 µm. All observations in Figure S1A,B, were confirmed with three experimental replicates.

(C) Line scan histogram profiles through Figure 1B,C,E demonstrate that MAD2L2 protein (green profiles) does not colocalize with compact DNA, and the heterochromatin markers H3K9me2, H3K27me3 and HP1alpha (red profiles).

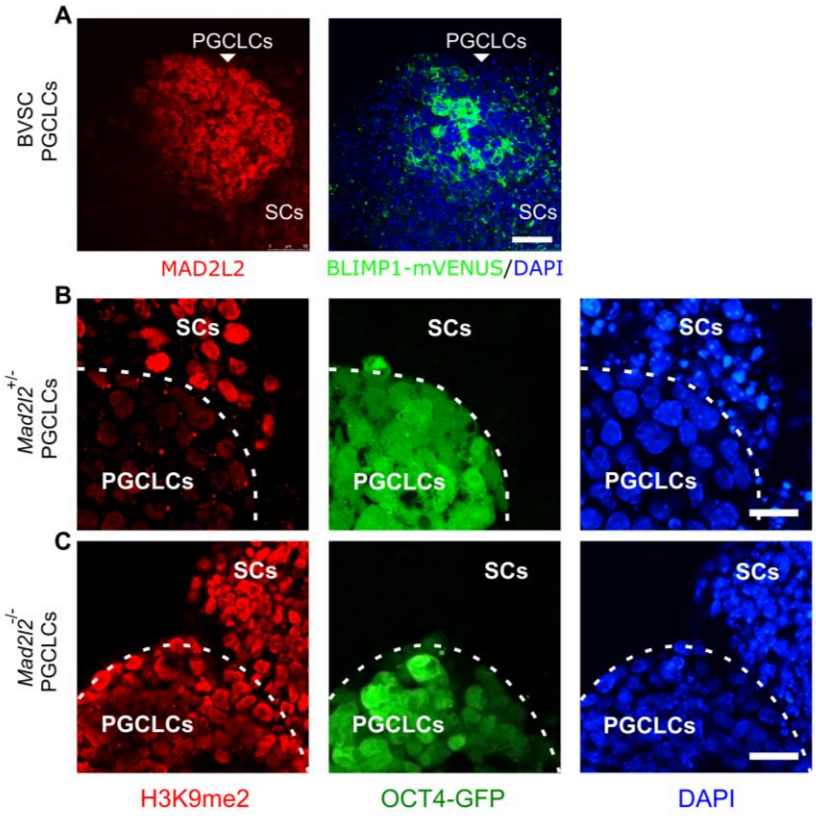

Figure S2 (Related to Figure 3). *Mad2l2*-deficient PGCLCs Do Not Switch Their Histone 3 modifications

(A) MAD2L2 expression in wild-type PGCLCs, which were identified by expression of a BLIMP1-mVenus transgene (Hayashi et al., 2011).

(B) Wild-type PGCLCs identified by an Oct4-GFP transgene have lost the expression of H3K9me2, while *Mad2l2*-deficient PGCLCs maintained high levels. H3K9me2 expression in GFP-negative, somatic cells (SCs) was not affected by the *Mad2l2* mutation.

Magnification bars = 50 μm (A), = 25 μm(B).

All observations were confirmed with three experimental replicates.

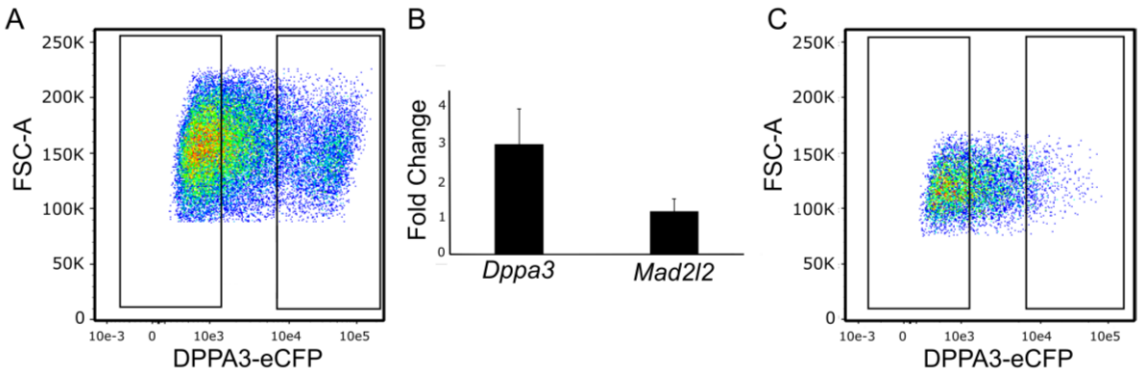

Figure S3 (Related to Figure 3). Recovery of Dppa3 and Mad2l2 expression

(A) BVSC-ESCs grown in LIF/2i medium were sorted into two populations based on the high or low expression of the *Dppa3-eCFP* transgene.

(B) In both populations the expression of *Dppa3* and *Mad2l2* were determined by qPCR. For each value, the average numbers from three independent experiments were calculated. These data confirm a positive correlation between *Mad2l2* and *Dppa3* expression. Standard deviations were calculated based on three experimental replicates.

(C) DPPA3-eCFP-negative ESCs were recultured for 24 hours in LIF/2i. FACS analysis revealed that a fraction of cells had re-established expression of the DPPA3-eCFP transgene. These data suggest that also *Mad2l2* expression was recovered.

To separate negative and positive cells, two gates were placed based on a control negative cell line to the far left side for the negative cells and to the area in the right site with zero cell population for the positive cells.

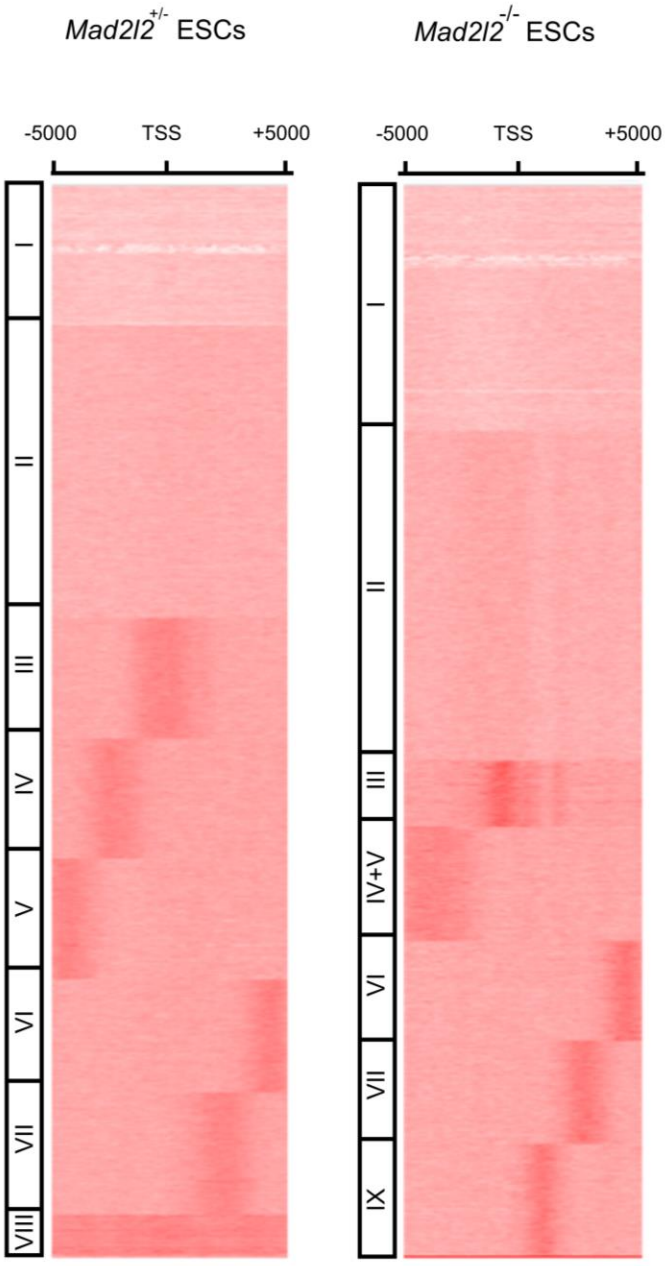

Figure S4 (Related to Figure 4). Perturbed Methylation Patterns Around the Transcriptional Start Sites in The Genome of Mutant ESCs

The distribution of 5mC between position -5000 bp and +5000 bp around the transcription start site were evaluated for 65.000 transcripts. Methylated regions were classified based on their distance from the transcription start sites. In Figure 4C the scans of class III regions for wild-type and *Mad2l2*-deficient ESCs are depicted. This observation was confirmed with three experimental replicates.

Legend for Supplemental Movie S1 (Related to Figure 1A)

The movie shows a 3D laser scan of MAD2L2 expression in one ESCs colony by confocal microscopy. Note that the antibody staining is on peripheral as well as internal cells, demonstrating that equal staining was obtained, and differences are not due to accessibility and penetration.